

2-2019

## Functionalized Carbon Nanotube Adsorption Interfaces for Electron Transfer Studies of Galactose Oxidase

Mulugeta B. Wayu

Michael J. Pannell

Najwa Labban

William S. Case

Julie A. Pollack

*See next page for additional authors*

Follow this and additional works at: <https://scholarship.richmond.edu/chemistry-faculty-publications>

 Part of the [Inorganic Chemistry Commons](#)

This is a pre-publication author manuscript of the final, published article.

---

### Recommended Citation

M. Wayu, M. Pannell, N. Labban, W. Case, J. Pollock, and M.C. Leopold, "Functionalized Carbon Nanotube Adsorption Interfaces for Electron Transfer Studies of Galactose Oxidase," *Bioelectrochemistry* 2019, 125, 116-126. DOI: <https://doi.org/10.1016/j.bioelechem.2018.10.003>

This Post-print Article is brought to you for free and open access by the Chemistry at UR Scholarship Repository. It has been accepted for inclusion in Chemistry Faculty Publications by an authorized administrator of UR Scholarship Repository. For more information, please contact [scholarshiprepository@richmond.edu](mailto:scholarshiprepository@richmond.edu).

---

**Authors**

Mulugeta B. Wayu, Michael J. Pannell, Najwa Labban, William S. Case, Julie A. Pollack, and Michael C. Leopold

# Functionalized Carbon Nanotube Adsorption Interfaces for Electron Transfer Studies of Galactose Oxidase

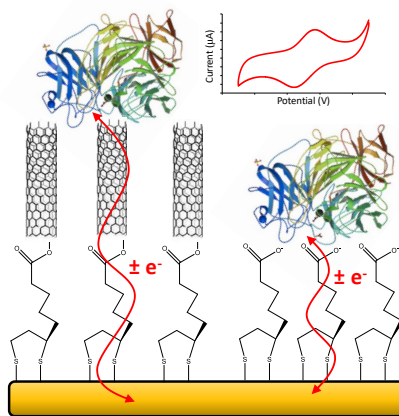
Mulugeta B. Wayu, Michael J. Pannell, Najwa Labban, William S. Case,<sup>†</sup> Julie A. Pollock,  
and Michael C. Leopold\*

*Department of Chemistry, Gottwald Science Center, University of Richmond, Richmond, VA 23173*  
*<sup>†</sup>Department of Biology, Chemistry, and Physics, Converse College, Spartanburg, SC 29302*

## Abstract

Modified electrodes featuring specific adsorption platforms able to access the electrochemistry of the copper containing enzyme galactose oxidase (GaOx) were explored, including interfaces featuring nanomaterials such as nanoparticles and carbon nanotubes (CNTs). Electrodes modified with various self-assembled monolayers (SAMs) including those with attached nanoparticles or amide-coupled functionalized CNTs were examined for their ability to effectively immobilize GaOx and study the redox activity related to its copper core. While stable GaOx electrochemistry has been notoriously difficult to achieve at modified electrodes, strategically designed functionalized CNT-based interfaces, cysteamine SAM-modified electrode subsequently amide-coupled to carboxylic acid functionalized single wall CNTs, were significantly more effective with high GaOx surface adsorption along with well-defined, more reversible, stable ( $\geq 8$  days) voltammetry and an average ET rate constant of  $0.74 \text{ s}^{-1}$  in spite of increased ET distance - a result attributed to effective electronic coupling at the GaOx active site. Both amperometric and fluorescence assay results suggest embedded GaOx remains active. Fundamental ET properties of GaOx may be relevant to biosensor development targeting galactosemia while the use functionalized CNT platforms for adsorption/electrochemistry of electroactive enzymes/proteins may present an approach for fundamental protein electrochemistry and their future use in both direct and indirect biosensor schemes.

## Graphical Abstract



**Keywords:** galactose, galactose oxidase, carbon nanotube, protein monolayer electrochemistry, cyclic voltammetry of adsorbed enzyme, enzyme activity

\*To whom correspondence should be addressed. Email: [mleopold@richmond.edu](mailto:mleopold@richmond.edu); Phone: (804) 287-6329 (MCL).

## 1. Introduction.

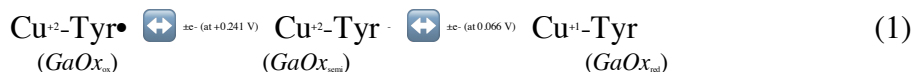
Protein monolayer electrochemistry (PME) [1, 2], where biomolecules are immobilized at modified electrodes, remains an effective strategy for studying fundamental electron transfer (ET) properties of biological systems including mitochondrial respiration and photosynthesis [3] as well as those with implications for biosensor design [4, 5], bioseparations [6], bioelectrocatalysis [4, 5], and biocompatible materials [7]. Early PME work focused on self-assembled monolayer (SAM) modified electrodes as a highly ordered, tailorable interfaces to which electroactive heme-based cytochromes (*e.g.*, cyt c, cyt b5) [2], copper “blue” proteins such as azurin [8], and other enzymes/proteins were adsorbed and electrochemically studied. By mimicking the protein’s natural adsorption partner (*i.e.*, important protein-protein complexes) [9-11], the PME approach isolates the ET reaction and enables potentiostatic control over the free energy of the ET reaction, thereby facilitating the measurement of important thermodynamic and kinetic parameters such as formal potential, reorganization energy, and ET rate constants [3].

In recent years, PME continues to be utilized in conjunction with SAM-based platforms and other substrates to study a range of biomolecules. A significant portion of recent literature features PME strategies focusing on cyt c electrochemistry at a variety of different adsorption platforms including electrostatic and covalent attachment at thiol-based SAMs [9, 12, 13], phosphonic acid functionalized indium tin oxide (ITO) electrodes [14], and lipid membrane coatings on glass carbon electrodes [15]. Similar platforms, alkylsilane modified ITO [16] and hydroxyl-terminated SAMs [17], have been employed in recent studies on azurin as well. The goals of most of these studies are to investigate ET or adsorption kinetics [14], ET distance dependence [18], or reorganization energy of a system [19]. Additionally, recent reports show PME strategies being used to study enzymes including glucose oxidase (GOx) [12] and urease [14]. Armstrong *et al.* used diazonium coupling to covalently modify and attach laccase metalloenzymes and Bernhardt *et al.* showed coadsorbed sulfite dehydrogenase within a polymer matrix with each study showing electrocatalytic behavior [20, 21]. In many of these cases, the PME strategy allows for the study of enzymatic behavior at synthetic interfaces that may be relevant to the future design of first generation biosensors [22, 23].

Within PME studies emerges a subcategory approach that incorporates nanomaterials into the modified electrode to promote biomolecule ET of adsorbed interfacial molecules. In some

cases, the ET of cyt c and azurin have been successfully studied at films of gold nanoparticle (NP) [3, 24] where information gleaned from the fundamental study eventually informed the similar electrode modifications for biosensor designs [25]. Additionally, there are literature reports of electrodes being modified with carbon nanotubes (CNTs) that are ultimately utilized in sensor designs [26-28]. In some of these cases, the CNTs were incorporated into composite films, sometimes including metal-oxide nanoparticles and/or enzymes, for the purpose of harnessing their conductivity or electrocatalytic activity to enhance sensitivity during targeted sensing [27, 29-31]. Minter *et al.* used anthracene modified MWCNTs as direct ET scaffolds for laccase electrochemistry [32]. Lojou and coworkers used single-walled CNTs (SWCNTs) and SAM junctions to immobilize Ni-Fe hydrogenase with a predominant specific orientation in order to explore electrocatalytic properties, noting that direct ET was hindered at long chain SAMs [33].

While PME strategies have been effective for certain proteins (*e.g.*, cyt c, azurin), their successful application to other biomolecules has been more rare. In particular, examples of the direct ET for the copper-containing enzyme galactose oxidase (GaOx) have been particularly scarce. The enzyme itself is a metalloenzyme (9.8 x 8.9 x 8.7 nm) consisting of three domains, a copper redox center buried only 8 Å from the surface of the molecule [4], and no co-factors. The ET reaction of GaOx occurs in a two electron step ( $n = 2$ ) with the initial reduction  $E^{\circ'}$  of fully oxidized tyrosine radical in the active site ( $\text{Cu}^{+2}\text{-Tyr}^{\bullet}$ ) to form a semi-oxidized intermediate species ( $\text{Cu}^{+2}\text{-Tyr}^-$ ) followed by the fully reduced state ( $\text{Cu}^{+1}\text{-Tyr}$ ) [4]:



Note:  $E^{\circ'}$  values reported vs. Ag/AgCl (KCl<sub>sat</sub>)

A review in 2005 affirms that direct ET of GaOx at an electrode had yet to be established even though the enzyme showed high reactivity with other redox partners and offers this relatively easy access to its active site in a manner similar to cyt c [34]. At the time, Tkac and coworkers [35] demonstrated irreversible cyclic voltammetry (CV) of GaOx at bare gold electrodes but attempts by Haladjian *et al.* [36] to observe GaOx electrochemistry at short chain SAMs (*e.g.*, aldrithiol) resulted in poorly defined cyclic voltammetry that was unstable over time, indicating a strong, destabilizing interaction between the enzyme and the gold surface [34]. Attempts to use

longer-chain SAMs in order to minimize GaOx-gold interactions, including SAMs comprised of decanethiol, mercaptoundecanoic acid (MUA), and 11-amino-1-undecanethiol, did stabilize the SAM background but failed to produce voltammetric peaks during normal CV analysis. At these longer-SAM interfaces, only the use of differential pulse voltammetry (DPV) resulted in observable peaks consistent with the peak potentials of GaOx [34]. Voltammetry that clearly defines the two-electron transfer, however, was not observed in these experiments.

Schiffrin and coworkers contributed a seminal report regarding direct ET study of GaOx by employing a gold-NP-SAM modified electrode for the immobilization of the enzyme [4]. With a dithiol SAM modified gold electrode, thioctic acid (TA) protected gold NPs with diameters of 1.4 ( $\pm 0.3$ ) nm were covalently attached *via* thiol linkages at the interface before the subsequent adsorption of GaOx. The design strategy of the Schiffrin electrode modification was to achieve reversible ET of GaOx *via* direct coordination of carboxylic acid functional groups on the NP with the Cu(II) center active site of the enzyme *via* ligand replacement of coordinated water molecule. Cyclic voltammetry of GaOx adsorbed at this system revealed voltammetric peaks that became more defined with background subtraction and were consistent with the two electron transfer of the enzyme. Formal potentials ( $E^{\circ'}$ ) of 0.241 V and 0.066 V (vs. Ag/AgCl (KCl<sub>sat</sub>)) were obtained *via* peak deconvolution for the Tyr•/Tyr and Cu<sup>I/II</sup> redox couples, respectively (see Reaction 1, above). As is the case with many metalloenzymes or metalloproteins, the  $E^{\circ'}$  of the enzyme's copper metal couple is shifted from that of uncoordinated, aqueous copper ( $\sim +0.040$  V vs. AgCl (KCl<sub>sat</sub>)). Surface coverage ( $\Gamma$ ) the author's claim as consistent with that of a protein film were calculated from charged passed during a two-electron reaction ( $n=2$ ) and the observed electrochemistry was stable for up to one day in the study [4].

In this paper, the direct ET of native GaOx adsorbed at interfaces without specific orientation or requiring a surrounding matrix is explored at both traditional SAM-modified gold electrodes, classic protein electrochemistry platforms, and at SAM platforms modified further with functionalized CNTs *via* amide coupling chemistry. While both of these interfaces allow for stable cyclic voltammetry with well-defined peaks, the successful incorporation of CNTs allows for greater ET distances without loss of kinetics and more in-depth probing of the active site of GaOx. Traditional protein electrochemistry thermodynamic and kinetics parameters are compared between the two systems as well as with alternative adsorption platforms found in the literature.

This study represents a strategy for studying fundamental ET reactions of GaOx at a synthetic interface. Unlike prior studies which show site-mutation results in loss of enzyme activity [37], results from the presented scheme show that enzyme function is maintained at the optimized CNT interface. Thus, this study may be relevant to the future development of any 1<sup>st</sup> generation biosensors that require electrochemically active, stable metalloenzyme activity confined to electrodes, particularly for development of galactose biosensors for galactosemia diagnosis [38].

## 2. Experimental Details.

**2.1 Chemicals and Instrumentation.** Unless otherwise stated, all chemicals were purchased reagent grade or higher from Sigma-Aldrich, including GaOx from *Dactylium dendroides*, and used as received. Functionalized CNTs were purchased from Nano Labs (Waltham, MA). All solutions were made with 18 M $\Omega$ ·cm ultra-purified water (PureLab-Ultra, Elga). Electrochemical measurements were performed with CH Instruments potentiostats (Models 1000B and 420B). Inverted electrochemical “sandwich” cells, described and used in previous studies of this nature by our laboratory [3, 24] and others [1], feature a Ag/AgCl (KCl<sub>sat</sub>) reference electrode (Microelectrodes, Inc.), a platinum wire counter electrode, and an evaporated gold film substrate (Evaporated Metal Films Corporation) as a working electrode (0.32 cm<sup>2</sup>).

**2.2 Substrate Preparation, Modification, Film Assembly and Characterization.** The gold working electrodes were electrochemically cleaned in 0.1M H<sub>2</sub>SO<sub>4</sub> and 0.01M KCl solution as previously described [3, 24] before being exposed to a thiol (SAM) or mixed thiol (mixed SAM) solution in ethanol for 24 hours to allow for SAM formation. The SAM-modified gold substrates were rinsed thoroughly with ethanol, NP water, and 4.4 mM potassium phosphate buffer (PB) at pH 7 before electrochemical characterization of the film. Dithiol SAM and carboxylic acid SAM modified substrates were further modified with in-house synthesized gold NPs *via* exposure to either a solution of TA-protected gold NPs (avg. diameter ~10 nm) or successive solutions of poly-L-lysine (PLL) cationic linkers followed by citrate-stabilized (CS) gold NPs, respectively and as previously described [39].

Films designated for subsequent amide coupling with CNTs were then exposed to 500  $\mu\text{L}$  of a solution of functionalized CNTs suspended in 50 mM MES buffer (1 mg/mL, pH 6.00). More specifically, electrodes modified with thioctic acid (TA) SAMs were exposed to amine-functionalized CNTs, while the substrates modified with a cysteamine SAMs were exposed to carboxylic acid-functionalized CNTs. Amide coupling between the SAMs and the CNTs was accomplished by adding 120  $\mu\text{L}$  of 200 mM aqueous hydroxysulfosuccinimide (Sulfo-NHS) and 12  $\mu\text{L}$  of 200mM aqueous *N*-Ethyl-*N'*-(3-dimethylaminopropyl)carbodiimide hydrochloride (EDC) to the cell chamber and allowing them to react for another 24 hours [40]. The CNT augmented films were electrochemically characterized prior to GaOx adsorption from an enzyme solution (1 mg/mL in 20 mM 2-(*N*-morpholino)ethanesulfonic acid (MES) buffer, pH 5.1) for 1 hour. The cells were rinsed thoroughly and refilled with supporting electrolyte (20 mM MES buffer, pH 7.5) prior to conducting GaOx ET studies using (CV, DPV). As previously shown [3, 24], apparent ET rate constants ( $k_{\text{et}}^{\text{app}}$ ) were determined by applying Laviron's simplest model [41] for an adsorbed species where a charge transfer coefficient of 0.5 is assumed and the adsorbed voltammetry is collected at increasing sweep rates to achieve quasi-reversible peak splitting ( $\geq 200$  mV). A hydrogen peroxide fluorescence assay (Sigma-Aldrich) was used to assess adsorbed GaOx activity. All experiments examining GaOx activity in enzymatic metabolism of galactose substrate were conducted with buffers pre-treated with catalase-agarose beads to remove residual hydrogen peroxide.

Cross-sectional transmission electron microscopy (TEM) was performed with a previously established procedure [24]. Briefly, SAM-modified gold electrodes subsequently amide-coupled to CNTs were attached to clean microscope slides using Embed 812 epoxy resin (EMS) before a resin-filled "00" BEEM capsule was inverted onto the film and allowed to cure (18h; 60°C). After cooling to room temperature, the mounted slides were thermally shocked on a hot plate (20s; 200°C) to facilitate removal of the blocks containing en face films. A jeweler's saw was used to remove a thin layer of the block containing the CNT film, which was subsequently embedded in a flatmold using additional resin (film side facing the interior of the well) before using a Leica UCT ultramicrotome diamond knife (Diatome) to section the sample, film perpendicular to the knife's edge. Sections were collected on carbon-coated Formvar grids (EMS) for TEM imaging (JEOL

1010). Ellipsometry measurements for film thickness were made using a VASE ellipsometer (J.A. Wollam).

### 3. Results & Discussion.

#### 3.1 GaOx at SAM-modified Electrodes.

Three different short-chain SAM-modified gold electrodes were exposed to GaOx solutions in order to facilitate immobilization of the enzyme and subsequent ET study. Electrodes were modified with SAMs comprised of one of the following types of thiols: 4-mercaptoaniline (4-aminothiophenol), 2-mercaptoethylamine (cysteamine) or Mercaptoethylaminecystamine, or  $\alpha$ -lipoic acid (thiotic acid). **Figure 1 (inset)** represents the schematic (thiotic acid example shown) believed to be representative of the SAM-based adsorption platforms. As in prior studies [3], with all of these systems, double-layer capacitance ( $C_{dl}$ ) can be used to verify effective cleaning of gold followed by thiol attachment and SAM formation *via* a significant decrease in  $C_{dl}$ . Similarly, voltammetry of potassium ferricyanide (FeCN) at these interfaces can also be used to characterize the films with attenuated peaks indicating the presence of a low-defect, blocking SAM. An example of this type of characterization is shown in Supporting Information (Fig. SI-1) for the thiotic acid SAM (TA-SAM) modified system, but similar results were collected for the 4-aminothiophenol SAM (4-ATPh SAM) and the cysteamine SAM (CYST-SAM) – results not shown.

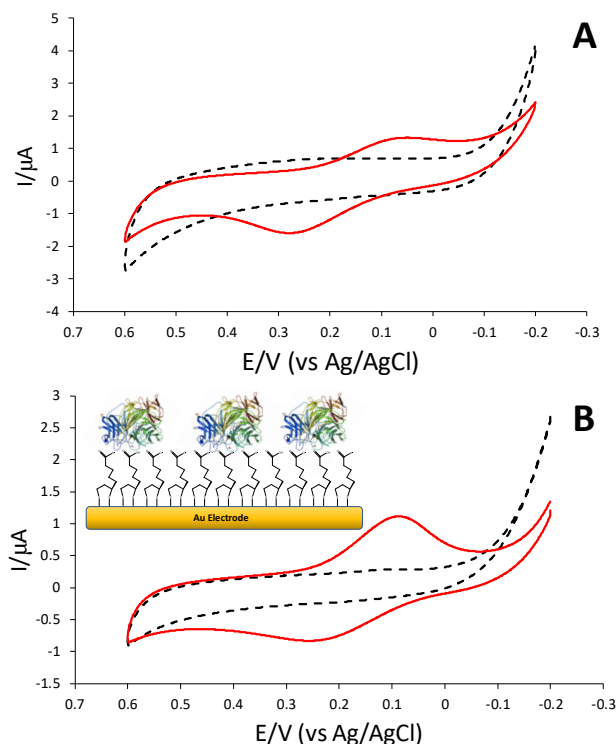


**Figure 1.** Typical cyclic voltammetry of GaOx adsorbed at (A) cysteamine SAM and (B) TA-SAM modified electrodes with background (SAM only; dashed trace) overlay in 20 mM MES buffer (pH 7.5) at a scan rate of 0.020 V/sec. **Inset:** Schematic representation of adsorbed GaOx monolayer at a TA-SAM modified gold electrode for fundamental ET studies. Note: GaOx adsorbed to CYST-SAM modified electrodes (not shown).

After verifying the presence of these SAMs on the gold substrates, each interface was exposed to a GaOx solution in order to immobilize a layer of enzyme. Cells were subsequently rinsed of excess enzyme solution before being refilled with 4.4 mM PB at pH 7. **Figure 1** shows the resulting cyclic voltammetry of the various SAM platforms with and without adsorbed GaOx. The voltammetric peaks observed are attributed to the redox electrochemistry associated with the Cu core of the GaOx enzyme (Rxn 1, above). Both the CYST-SAM and the TA-SAM systems exhibit irreversible to quasi-reversible voltammetry at 20 mV/s that is suggestive of sluggish ET kinetics. GaOx at the 4-ATPh SAM showed only small, poorly defined voltammetric peaks consistent with low surface coverage of adsorbed protein (Supporting Information, Fig. SI-2). The resulting GaOx voltammetry at both the TA and CYST SAM systems consistently shows a single, broadened, voltammetric wave that, while observed in prior reports [34], is *not* consistent with the expected two-electron transfer process for GaOx. The observed voltammetry must be considered a convolution of two separate but unresolved peaks from the Tyr<sup>•</sup>/Tyr and Cu<sup>+1/2</sup> redox couples of GaOx [4]. As such, electrochemical parameters must be estimated and compared relatively. All the estimations and measurements of the relevant apparent electrochemical parameters for GaOx adsorbed to these SAM systems as well as bare gold are shown in **Table 1**, including apparent

GaOx surface coverage ( $\Gamma$ ), apparent full-width-at-half-maximum (FWHM) of the voltammetric peak, and estimations of apparent ET rate constants. While the peaks remained unresolved for the two electron transfer of GaOx, it is notable that the apparent formal potentials are consistent with the midpoint of the only study that reports resolved peaks for the two-electron transfer (0.153 V) [4]. Unlike other studies of GaOx at SAM interfaces [34] that see single voltammetric peaks, however, the voltammetry observed herein has clearly defined oxidation and reduction waves. Additionally, the apparent ET rate constant calculated for these systems is consistent with those reported in the literature (0.6-0.9 s<sup>-1</sup>) including systems using longer chain SAMs (e.g., biphenyl-4,4'-dithiol) with nanoparticles at the interface [4]. A small decrease in rate is observed comparing the GaOx adsorbed at bare gold versus all the SAM platforms (Table 1), an effect expected with the modification of the gold with the short-chain SAMs.

The lack of reversibility at these short-chain SAMs is consistent with prior reports [34] and reflective of what is thought to be poor electronic coupling between the SAM interface and the enzyme's redox active site that results in slower ET kinetics. Additionally, even though two of the short-chain SAMs allowed for observable adsorbed electrochemistry from the GaOx, such interfaces can still have exposed gold at defect sites and risk GaOx denaturation from biomolecule exposure to gold [4]. The higher than expected values of  $\Gamma$  for these systems are thought to be partially attributable to the inability of the adsorption platform and voltammetry technique to resolve the peaks for the two electron process as well as peak broadening - measured as apparent FWHM (Table 1) and attributed to the different orientations of adsorbed GaOx enzyme. Both of these effects contribute to convoluted peaks that likely increase the measured charge that is used to calculate surface coverage. Additionally, charge discrimination is more challenging for adsorbates at short-chain SAMs which have higher dielectric layers compared to longer-chain, more insulating, alkanethiolate films.

In prior PME reports [1], the use of two-component or mixed SAMs has had significant impact on improving the electronic coupling of the adsorbed protein to the SAM interface. Mixed SAMs formed with a base SAM of TA and various diluent thiols, including 11-mercaptoundecanoic acid (MUA), 11-mercaptoundecanol (MUD), 8-octanethiol (C8), and 6-mercaptohexanol (MHOL) that were all tested for improved GaOx adsorption and subsequent ET properties. In all cases, voltammetric peaks attributable to GaOx ET were either not observed or

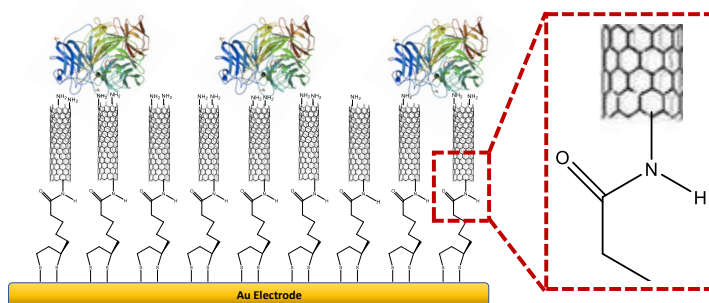
barely discernable over background. Mixed SAMs comprised of 6-mercaptopentaonic acid (MHA) exchanged with diluents of MUA, MHOL, and MUD showed only marginal improvement in the observed voltammetry and an order of magnitude slower  $k_{\text{et}}$  for most of the systems tested (see Table SI-2, Supporting Information). Collectively, these results suggest that SAM adsorption platforms are clearly limited in their ability to allow for GaOx ET studies and are susceptible to stability issues (see below).

As previously mentioned, an alternative adsorption platform that has found success in other protein/enzyme ET studies are interfaces featuring different kinds of alkanethiolate-protected or electrostatically stabilized gold NPs [3, 24, 42]. In the current study, various gold NP modified electrode systems were tested as GaOx adsorption interfaces including dithiol-SAMs with covalently attached TA-stabilized gold NPs and carboxylic acid-SAM modified electrodes subsequently modified with cationic linking polymers [3] to connect CS-stabilized NPs. Electrochemical analysis of GaOx adsorbed at these interfaces is summarized in Table SI-3 (Supporting Information). In general, this analysis did not result in well-formed voltammetry, and the results were not significantly improved from those achieved at SAM interfaces (Table 1). While the NP platform did not produce a substantial effect in the GaOx adsorption and electrochemistry, we note that the NPs used in this study are significantly larger ( $d \sim 10$  nm) than those used in a prior study ( $\sim 1.5$  nm diameter). In that study, TA-stabilized NP interfaces allowed for greater electronic coordination with the GaOx redox center [42]. Given that conclusion, the observed results are not entirely surprising.

### **3.2 GaOx at CNT-coupled SAM-modified Electrodes.**

Functionalized CNTs were envisioned as an advantageous addition to the SAM-based adsorption platforms as they offer high conductivity, tailorable size/functionality, and greater masking of the gold electrode from biological adsorbates. With this last attribute, a potential disadvantage is an increase in distance and subsequent ET kinetics decay from GaOx to the electrode. Four different types of CNTs were used to supplement the established SAM-modified electrodes: multi-wall (MW) and single wall (SW) amine-functionalized CNTs ( $\text{NH}_2$ -MWCNT and  $\text{NH}_2$ -SWCNT) as well as single and multi-wall carboxylic acid-functionalized CNTs ( $\text{COOH}$ -

SWCNT and COOH-MWCNT). The average outer diameters were  $\sim 1.5$  and  $\sim 9.5$ - $13$  nm for the functionalized SWCNTs and MWCNTs, respectively. Prior characterization of these materials has shown that the functional groups are predominantly found on the ends of the CNTs [43]. The carboxylic acid functionalized materials were selected for amide-coupling to the CYST-SAM, allowing for a carboxylic acid adsorption interface with GaOx, whereas the amine-terminated CNTs, once amide-coupled to the TA-SAM, should yield an amine dominated adsorption interface. **Scheme 1** represents a schematic graphic of the proposed adsorption platform with an emphasis on the connectivity and functionality of interfaces (*e.g.*,  $\text{NH}_2$ -SWCNTs amine-coupled to a TA-SAM). In a similar fashion, reversing the functionality of the coupling, COOH-CNTs can be amide-coupled to a CYST-SAM as well. It should be noted that the CNTs are not vertically aligned and are likely more randomly and laterally dispersed (see below).



**Scheme 1.** Schematic representation of GaOx adsorbed to a  $\text{NH}_2$ -SWCNT amide-coupled (**inset**) to a TA-SAM modified gold electrode for fundamental ET studies. Notes: CNTs are depicted in vertical order to emphasize amide coupling and functionality of interfaces; GaOx was also adsorbed to COOH-CNT interfaces amide-coupled to CYST-SAM modified gold electrodes, reversing the direction of the amide linkage (not shown).

The different CNTs were covalently attached to their respective SAMs *via* an amine-coupling reaction within the electrochemical cell chamber (see Experimental Details). The successful attachment of CNTs to the SAM-modified electrodes was verified prior to GaOx adsorption through two primary electrochemical methods,  $C_a$  measurements and ferricyanide redox probing. Electrochemical confirmation was employed so that there was minimal disruption of the films, including not requiring removal of the gold electrode from the electrochemical cell. As shown in previous reports [3],  $C_a$  measurements of clean bare gold substrates followed by subsequent CYST-SAM modification (before amide coupling of COOH-CNTs) show a substantial decrease in current with SAM formation, an effect attributed to an increase in distance of the electric double layer

between the solution and electrode as well as a decrease in the separating material's dielectric constant. **Figure 2A** compares capacitance scans of bare, CYST SAM-modified gold, and CYST-SAM after amine-coupling reactions with COOH-SWCNTs. Typical of clean gold being modified with any SAM, the  $C_{dl}$  decreases are consistent with a SAM comprised of short-chain functionalized thiols. As seen in other reports with CNTs at electrodes, the successful attachment of the COOH-CNTs results in a significant increase in  $C_{dl}$ , suggesting that the coupling of the CNTs was successful.

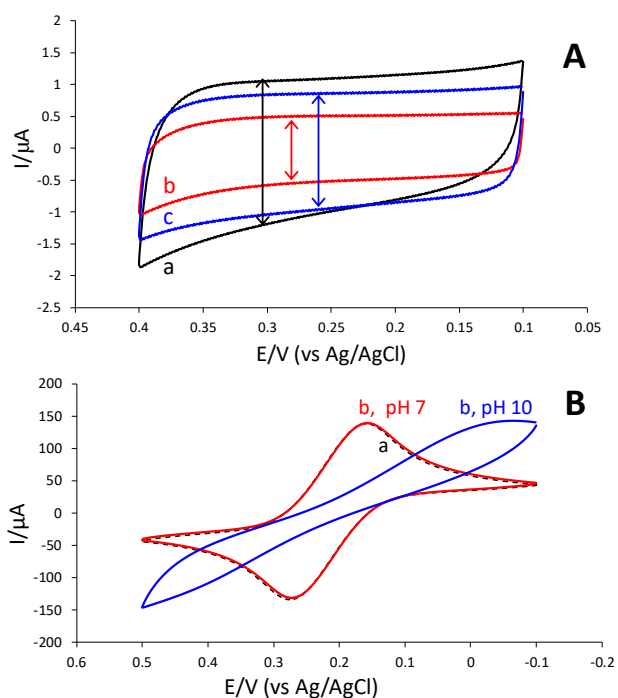


**Figure 2.** (A) Double-layer capacitance ( $C_{dl}$ ) background scans in 8 mM PB (pH 7) of (a) bare gold, (b) CYST-SAM modified gold, and (c) CYST-SAM modified gold after amide-coupling of COOH-SWCNTs; (B) cyclic voltammetry of 5 mM  $\text{Fe}(\text{CN})_6^{3-/4-}$  (0.5 M KCl) at (a) CYST-SAM modified gold, (b) CYST-SAM with amide-coupled COOH-SWCNT in PB at pH 7 and 10 (noted above). Note: scan rate is 0.020 V/sec.

If COOH-CNTs are successfully attached to the CYST-SAM, carboxylic acid groups, rather than amine groups, should now dominate the solution interface at the modified electrode. Cyclic voltammetry of FeCN (**Figure 2B**) at the CYST-SAM interface results in clearly defined, diffusional voltammetry suggesting the probe has relatively easy access to the underlying electrode. The same experiment after COOH-SWCNTs are amide coupled at the interface achieves the same result at a pH of 7. However, when the pH of the FeCN solution is buffered at pH 10,

the carboxylic acid groups, if present, should be deprotonated and result in a negatively charged electrode interface that easily repels or blocks the negative redox probe's approach. Blocked cyclic voltammetry is observed under these conditions (Fig. 2B), reinforcing the  $C_{dl}$  results that suggest the presence of COOH-SWCNTs at the interface. The same experiment conducted with DPV reveals the same result as well (Supporting Information, Fig. SI-3).

In a similar manner, successful amine coupling of  $\text{NH}_2$ -SWCNTs was verified at TA-SAM modified electrodes. **Figure 3** shows the  $C_{dl}$  and FeCN probing results for that system. Of note in this case, however, is that the  $C_{dl}$  results are not as suggestive of attachment of the  $\text{NH}_2$ -SWCNTs, with a much more subtle increase in  $C_{dl}$  after the amide coupling reaction (Fig. 3A). However, FeCN voltammetry is nearly completely blocked at the TA-SAM modified electrode but is restored to a well-defined diffusional shape upon attachment of the  $\text{NH}_2$ -SWCNTs (Fig. 3B). Once again DPV measurements of the same interfaces are consistent with the cyclic voltammetry results. Similar experiments were conducted to verify the successful attachment of functionalized MWCNTs at the TA and CYST-SAM modified electrodes (not shown). In all cases, the electrochemical results suggest successful attachment of the nanomaterials.

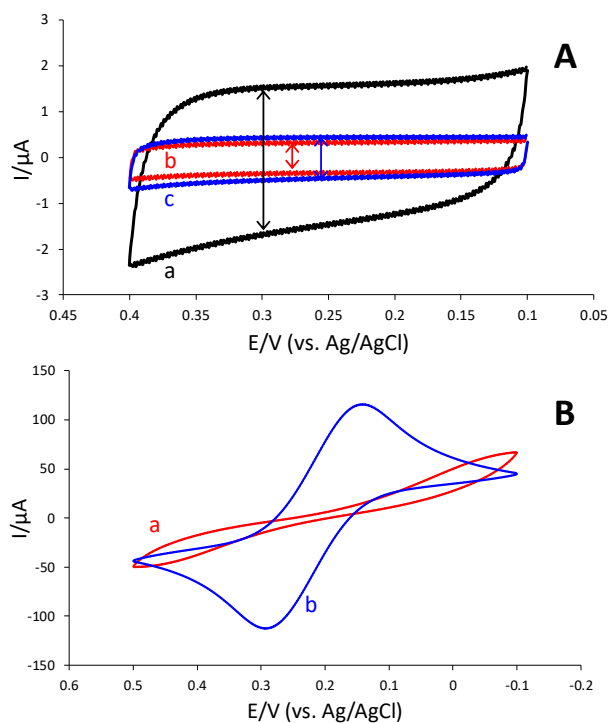


**Figure 3.** (A) Double-layer capacitance ( $C_{dl}$ ) background scans in 8 mM KPB (pH 7) of (a) bare gold, (b) TA-SAM modified gold, and (c) TA-SAM modified gold after amide-coupling of  $\text{NH}_2$ -SWCNTs; (B) cyclic voltammetry of 5 mM  $\text{Fe}(\text{CN})_6^{4-}$  (0.5 M KCl) at (a) TA-SAM modified gold, (b) TA-SAM with amide-coupled  $\text{NH}_2$ -SWCNTs. Note: scan rate is 0.020 V/sec.

It is of interest to compare the cyclic voltammetry of adsorbed GaOx at SAM and SAM-CNT platforms that offer the same functionality at the interface as well as each system's measured electrochemical parameters (**Figure 4** and **Table 1**). Within these results, a comparison of GaOx adsorbed voltammetry at a CYST-SAM versus a TA-SAM modified with NH<sub>2</sub>-MWCNT (both systems present amine functionalized interfaces for GaOx), reveals that the use of the NH<sub>2</sub>-MWCNT platform results asymmetric, nearly irreversible voltammetry that is on slightly more defined than that observed at the CYST-SAM (Fig. 4A). Additionally, the NH<sub>2</sub>-MWCNT platform yields a slightly lower apparent surface coverage and small decrease in apparent  $k_{\text{eff}}$  compared to the CYST-SAM (Table 1). The lower GaOx is deemed significant given that the addition of COOH-MWCNT is likely adding electroactive surface area that should allow for increased enzyme adsorption [28]. This result suggests that there is poor electronic coupling between the COOH-MWCNTs and the GaOx. When a similar platform featuring NH<sub>2</sub>-SWCNT coupled to a TA-SAM modified electrode is compared to the CYST-SAM (both amine functionalized interfaces, Fig. 4B), no substantive change in apparent surface coverage and a decrease in  $k_{\text{eff}}$  is still observed suggesting that decreasing the CNT diameter does not substantially improve electronic coupling.

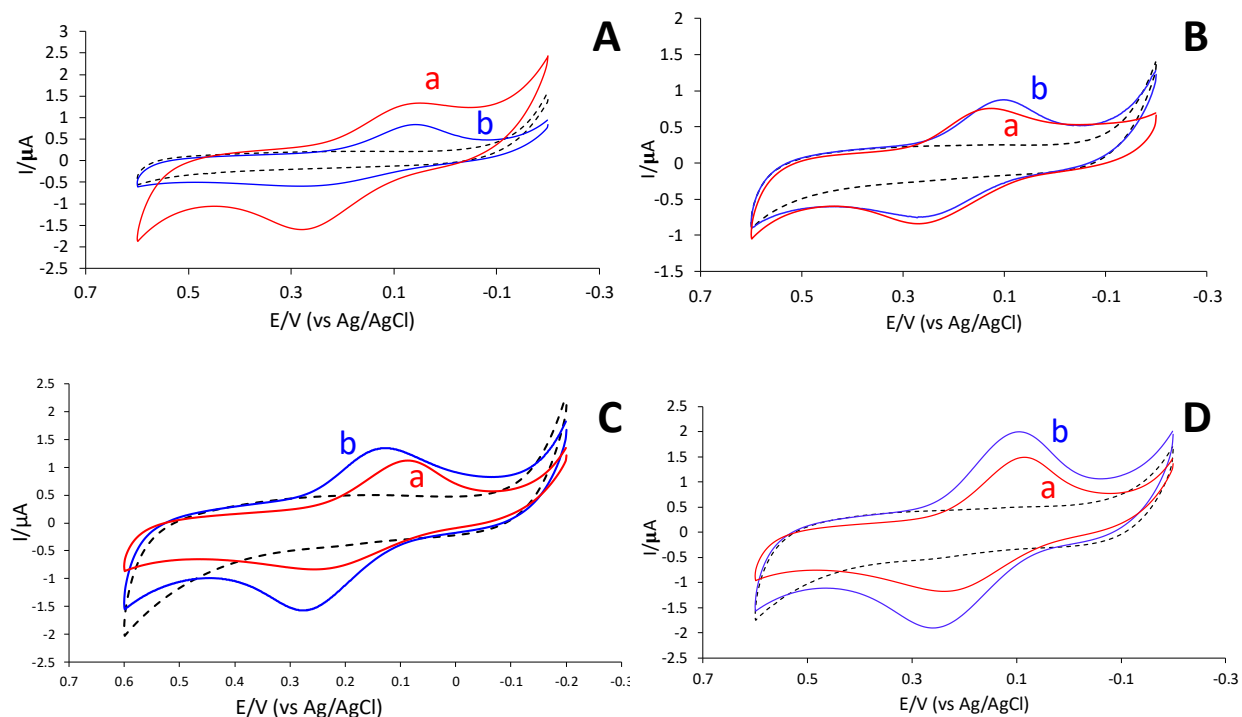


**Figure 4.** Typical cyclic voltammetry of adsorbed GaOx at (A) (a) CYST-SAM versus (b) TA-SAM with amide-coupled NH<sub>2</sub>-MWCNTs (both amine interfaces); (B) (a) CYST-SAM versus (b) TA-SAM with amide-coupled NH<sub>2</sub>-SWCNTs (both amine interfaces); (C) (a) TA-SAM versus (b) CYST-SAM with amide-coupled COOH-MWCNTs (both carboxylic acid interfaces) and; (D) (a) TA-SAM versus (b) CYST-SAM with amide-coupled COOH-SWCNTs (both carboxylic acid interfaces). Note: Voltammetry collected at scan rate of 0.020 V/sec in 20 mM MES buffer (pH 7.5); (SAM-CNT background, without adsorbed GaOx, dashed trace).

The voltammetry and ET properties of GaOx at a TA-SAM versus a CYST-SAM coupled with COOH-MWCNT (Fig. 4C) or COOH-SWCNT (Fig. 4D), where all the platforms present carboxylic acid-functionalized interfaces for GaOx adsorption, can also be compared. In this case, a smaller apparent surface coverage and a slight decrease in  $k_{\text{et}}^{\circ}$  are observed for the MWCNT films compared to the TA-SAM (Table 1). However, when COOH-SWCNTs coupled to a CYST-SAM serve as the interface for GaOx adsorption, apparent surface coverage remains similar to the TA-SAM but a nearly doubled  $k_{\text{et}}^{\circ}$  is recorded from voltammetry (Table 1) that is both more reversible and symmetrical (Fig. 4D). It should be noted that higher than expected GaOx surface coverage is measured at these platforms, a result likely related to the inability to resolve voltammetric peaks for the two electron transfer process (convoluted peaks), an increase capacitive background with the addition of CNTs at the interface, and the well-established increase in electroactive surface area that is achieved with CNT-modified electrodes [28] – all of which are factors leading to both artificial and real increases in charge measurements subsequently used for calculation of surface coverage. The inability of the platform to resolve the voltammetry of the two-electron process may also be related to the SWCNT interface allowing for multiple orientations of adsorbed enzyme – an effect that can increase the full-width-half maximum of voltammetry and further obscure to accurately integrate for charge (Table 1) [2,10].

These results suggest details about the binding of GaOx to synthetic interfaces with important implications. The COOH-SWCNT interface is distinct from the other nanomaterial platforms in that the interface offers a carboxylic acid moiety connected to a SWCNT that is smaller in diameter (~1.5 nm) compared to its multi-walled analog with a diameter of ~9.5-13 nm. In using the smaller diameter, functionalized CNT, we observe similar coverage to the TA SAM platform but a faster  $k_{\text{et}}^{\circ}$  even though we have substantially increased the ET distance between the enzyme and the electrode with the CNT film. The increase in ET distance can be visualized with cross-sectional TEM imaging, shown in **Figure 5**, which confirmed a thin film of SWCNTs comprises the adsorption interface (Additional imaging in Supporting Information, Fig. SI-4). The increase ET distance was further confirmed *via* ellipsometry measurements which determined the COOH-SWCNT/CYST-SAM films to be 2.33 ( $\pm 0.05$ ) nm in thickness versus the TA-SAM which, while too thin to be measured with the ellipsometry, are well-ordered films estimated to be only

~0.6 nm [24]. Even with a nearly 4-fold increase in the ET distance, which would typically result in decay, an increase in  $k_{\text{ET}}^{\circ}$  is observed – a result indicating that the COOH-SWCNT is better able to electronically couple the adsorbed GaOx through a specific interaction of the carboxylic acid moiety within the active site of the enzyme.

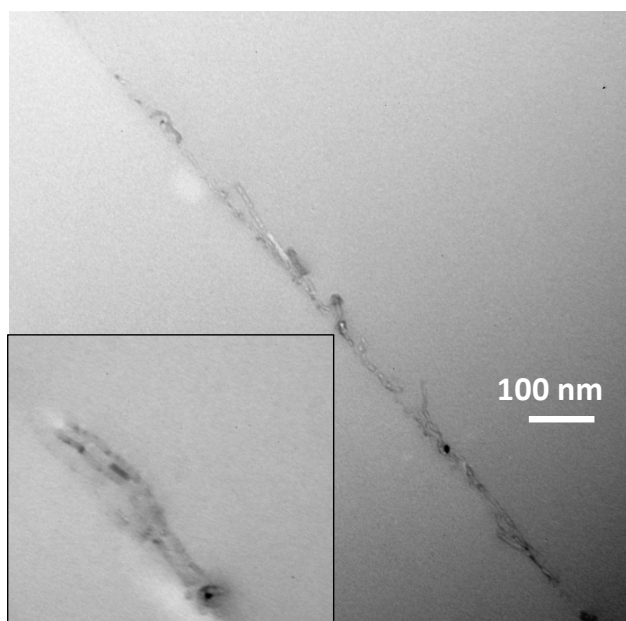


**Figure 5.** Cross-sectional TEM imaging of the COOH-SWCNT films that comprise the GaOx adsorption interface [80kV; 50000x]; **Inset.** Zoomed section of a film [80 kV; 75000x]. Notes: small black circles are believed to be CNT overlap (additional images of similar interfaces are included in Supporting Information (Fig. SI-4).

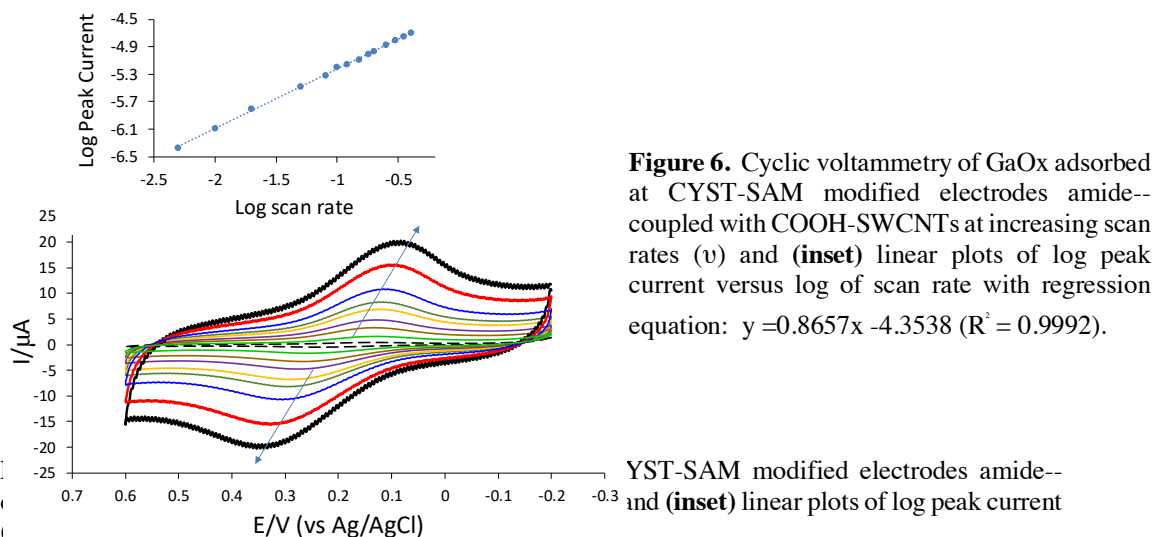
From their work with GaOx adsorbed at TA-modified gold NP interfaces, Schiffrin and coworkers, reporting similar  $k_{\text{ET}}^{\circ}$  values to this study (*i.e.*, 0.6-0.9 s<sup>-1</sup>) and also conclude two key observations that are relevant to the results herein. First, the diameter of their gold NP (~1.4 nm) is small enough to interact with the redox active site of GaOx. Second, the carboxylic acid functional group was determined to be critical in achieving more reversible adsorbed electrochemistry of GaOx – achieving direct coordination with the Cu(II) metal center active site *via* water replacement [42]. Taken collectively, we find our results, achieved with CNT adsorption platforms, to be consistent with that of the Schiffrin report. If the suggestion that effective electronic coupling is contingent upon the carboxylic acid coordination, then the GaOx voltammetry observed at the NH<sub>2</sub>-SWCNTs should follow suite as it is the correct size but lacks the carboxylic acid functionality. Indeed, in that case, a decrease in  $k_{\text{ET}}^{\circ}$  is observed (Table 1). Moreover, the COOH-MWCNT interface feature carboxylic acid moieties at tubes too large in

diameter (*i.e.*, ~9.5-13 nm) to interact effectively with the GaOx redox site and these platforms result in lower enzyme adsorption (Table 1).

The observation from the current study that incorporation of the CNT into the adsorption platform allows for greater distance independence of ET, without meaningful decay even over significantly greater distance, is an important finding of this study. Using the reported dimensions of the GaOx enzyme (0.8 nm minimum or 9 nm maximum ET distance) added to estimated or measured (TEM cross-section – see Fig. 5, for example) overall film thicknesses, estimations of ET distances in the systems are significantly larger for the CNT platforms compared to the SAM platforms (Table 1). In all the platforms, as expected, SAM modification of the gold electrode results in a modest decrease of ET rate. As a control, measurements of GaOx ET adsorbed to COOH-SWCNTs that have been dropcast on gold electrodes, *i.e.*, no SAM, exhibited slightly higher rate constant values (~2.0 s<sup>-1</sup>). This more effective independence of ET on distance for the adsorbed GaOx is attributable to the electronic properties of the incorporated CNTs. While their presence in the films does not necessarily enhance the ET rate, it does not show meaningful decay even when at ET distances is estimated to significantly greater (*i.e.*, peak separation and apparent ET rate constants do not reflect traditional distance decay as one would expect at SAMs of increasing chainlengths [24]. Taken collectively, the advantages of the CNT platforms, namely stability and more robust ET over distance, could have significant implications for incorporating the scheme into biosensor strategies, particularly if the system is able to maintain enzymatic activity.

Another major attribute of direct ET systems relevant for further development/applications is achieving greater stability. Prior work on GaOx direct ET reported instability [34] or short-lived stability of less than a day [4]. In this study, electrodes modified with CYST-SAM and coupled with COOH-SWCNTs represented the most effective adsorption platforms for GaOx, resulting in more reversible voltammetry of an apparent adsorbed species. An adsorbed species should show scan rate dependence where peak current is linearly proportional to scan rate rather than the square root of scan rate as would be the case for a diffusional species obeying the Randles-Sevcik equation [42, 44]. **Figure 6** displays the cyclic voltammetry of GaOx adsorbed at the COOH-SWCNT interface at increasing scan rates along with an inset of log peak current versus log scan rate. The linearity of the plot emphasizes the non-diffusional behavior of the GaOx at the interface. Similar

analyses were performed with the other CNT systems and also supported that GaOx exhibited adsorbed behavior (Supporting Information, Figs. SI-5-7).



Enzymes and proteins adsorbed directly to bare gold surfaces tend to denature and the risk of denaturation is only slightly mitigated with short chain SAM modified electrodes or short-chain monolayer protected gold NPs. This instability of adsorbed GaOx is demonstrated in the Schiffrin report where the GaOx voltammetry at the gold NP interface showed stability of only up to one day – though they do not define or show evidence of the instability observed [4]. Thus, the optimal adsorption platform would be an interface able to separate the enzyme from the gold surface, protecting it from metal surface induced denaturation, and maintain both high surface coverage and ET kinetics over time.

**Figure 7** tracks the apparent electroactive surface coverage and stability of GaOx adsorbed to bare gold, CYST-SAM, TA-SAM, and CYST-SAM amide coupled to COOH-SWCNTs over the course of eight days. Cyclic voltammetry of the adsorbed GaOx at the various systems was performed - integrating peaks at 0.020 V/s for surface coverage determinations each day. The surface coverage ( $\Gamma$ ) results show that the surface concentration of GaOx at the COOH-SWCNT interface starts high and remains relatively high over the course of the testing. Moreover, the cyclic voltammetry of this system, even after eight days, continues to display well-defined and

largely symmetrical voltammetric peaks (**Figure 8**). In particular contrast to the voltammetry of GaOx at the COOH-SWCNT is that of the enzyme at the CYST-SAM, which is nearly non-existent on the eighth day and registered less than 5 pmol/cm<sup>2</sup> of coverage by day two. Similarly, the

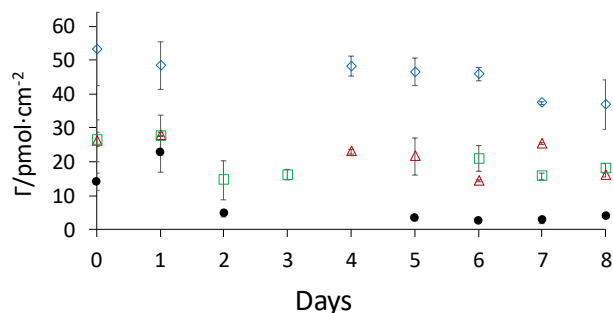


**Figure 7.** Stability tracking of surface coverage ( $\Gamma$ ) over days for GaOx adsorbed to bare gold ( $\Delta$ ), CYST-SAM modified gold ( $\bullet$ ), TA-SAM modified gold, and CYST-SAM modified gold coupled with COOH-SWCNTs ( $\diamond$ ). Note:  $\Gamma$  measured at 0.020 V/sec; in some cases, error bars are smaller than markers ( $n = 2-3$ ).

voltammetry of the enzyme at bare gold is drastically degraded on day eight compare the initial voltammetry (Supporting Information, Fig. SI-8). The comparison of the CYST-SAM system and the COOH-SWCNT system is striking and re-emphasizes the beneficial impact of using the CNTs

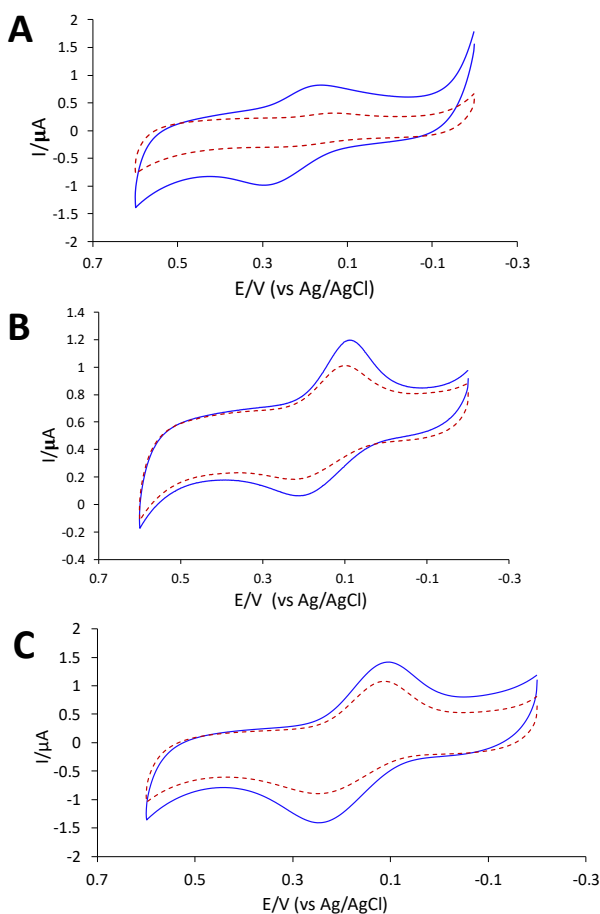


**Figure 8.** Comparison of representative cyclic voltammetry of GaOx adsorbed at day 0 (*solid, blue trace*) and day 8 (*red, dashed traces*) for GaOx adsorbed to (A) CYST-SAM modified gold, (B) TA-SAM modified gold, and (C) CYST-SAM modified gold coupled with COOH-SWCNTs. Notes: Scan rate is 0.020 V/sec; result of GaOx at bare gold is included in Supporting Information (Fig. SI-8).

as an adsorption interface. The reason for the degraded voltammetry over time is likely due to

both GaOx desorption off of the film and denaturation of still adsorbed GaOx – two processes that are difficult to completely experimentally differentiate. Desorption of GaOx from the interface is supported via fluorescence measurements (see below). Monitoring the apparent ET rate of GaOx over time for these systems reveals the general trend of an increasing rate constant over days of testing (Supporting Information, Fig. SI-9). GaOx adsorbed at the COOH-SWCNT/CYST-SAM/Au system and then rapidly exposed to temperatures that denature the GaOx while adsorbed at the interface show a corresponding increase in apparent  $k_{\text{ET}}^{\circ}$  observed in real-time (results not shown). Similarly, when GaOx that had been denatured overnight with heating to 90-95°C was adsorbed to the COOH-SWCNT/CYST-SAM/Au interface, an apparent  $k_{\text{ET}}^{\circ}$  of 2.12 ( $\pm 0.02$ )  $\text{s}^{-1}$  was measured, more than double that of native GaOx at the same interface (Table 1). In all of these experiments, however, the apparent surface coverage also decreases leaving open that the increase in rate is due to weakly or poorly coupled GaOx is desorbing and leaving GaOx with faster ET rates due to being more optimally adsorbed [45].

### 3.3 Adsorbed Enzyme Activity Assessment

A critical aspect any system that involves biomolecules immobilized on a synthetic platform is the preservation of enzyme structure and function. The results of this study thus far suggest that the CNT platforms are able to stabilize the adsorption and ET of GaOx but did not assess if the enzyme remains active at the interface – an important aspect if these materials are to be incorporated as functional components of future 1<sup>st</sup> generation biosensing schemes. While the system in this current study, a thin monolayer of enzyme, is appropriate for ET study, it significantly differs from biosensing films that target multi-layers of enzyme to produce a more robust signal. That said, confirmation of enzyme activity in the thin films serves as a precursor to those that see the combination of these materials as a viable strategy for building said multi-layers of GaOx for galactose biosensing. To confirm enzyme activity in the films studied here, a number of experiments were conducted. First, adsorption platforms were prepared as previously described above with the gold electrode modified with a CYST-SAMs coupled to COOH-SWCNTs ((Fig. 7d) and exposed to solutions of GaOx for 1-3 hours. The cells were then rinsed thoroughly and refilled with 500  $\mu\text{L}$  of buffer. Aliquots of 10  $\mu\text{L}$  were removed from the cell (control samples

without galactose) before adding 200  $\mu\text{L}$  of 10 mM galactose to each cell to facilitate the enzymatic reaction:



After only 5 minutes of galactose exposure, additional 10  $\mu\text{L}$  aliquots were removed from each cell and tested with the horseradish peroxide (HRP)-coupled fluorescent assay:

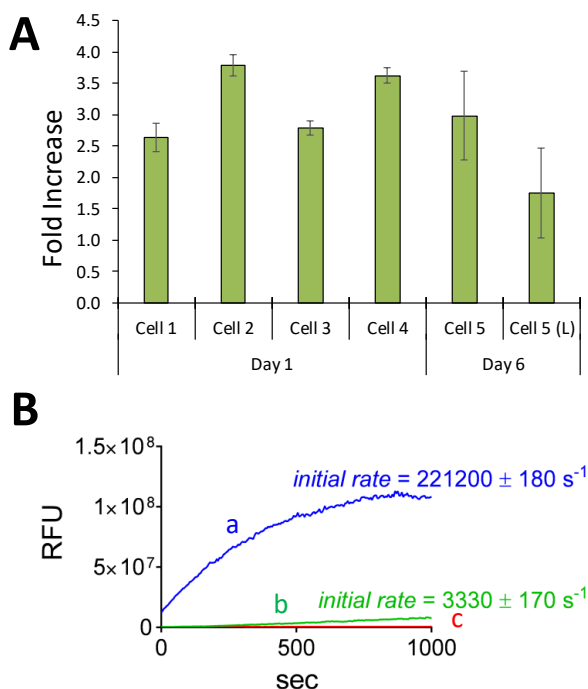
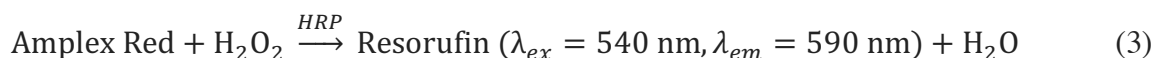


**Figure 9.** HRP-coupled fluorescence assay results for  $\text{H}_2\text{O}_2$  quantification from (A) aliquot sampling from the electrochemical cells with Au/CYST-SAM/COOH-SWCNT/GaOx systems where fold increase in GaOx activity 5 minutes after the addition of galactose substrate (200  $\mu\text{L}$  of 10 mM galactose) on Day 1 (Cells 1-4) and Day 6 (Cell 5), the latter including an additional measurement of the soaking buffer (L) and; (B) kinetic analysis for films of Au/CYST-SAM/COOH-SWCNT/GaOx coated over entire gold slides (area  $\sim 1.74 \text{ cm}^2$ ) with (a) native, (b) denatured, and (c) no adsorbed GaOx during exposure to 10 mM galactose substrate and tracking relative fluorescence units (RFU). Note: the films were run in duplicate ( $n=2$ ) and experiment repeated on films constructed within electrochemical cells (see Supporting Information).

The results, shown in **Figure 9**, show that solution from the cell after exposure to galactose expresses a consistent, approximately 3-fold increase in hydrogen peroxide production, an indicator of GaOx enzyme activity. An additional cell was prepared in a similar manner and allowed to sit with buffer over six days before an aliquot of this soaking buffer was removed and exposed to galactose. The cell was then thoroughly rinsed and re-exposed to new buffer before also being exposed to galactose (200  $\mu\text{L}$  of 10 mM galactose) as in the prior experiments. After 5

minutes, both aliquots were tested with the fluorescence assay where both the sample from the new buffer in the cell (Fig. 9, Cell 5) and the aliquot of the soaking buffer (Fig. 9, Cell 5 (L)) showed significant enzymatic activity of approximately 3 and 1.5 fold increase in activity, respectively, versus the same samples without galactose exposure. While these results reiterate the primary objective of the experiment (i.e., the adsorbed GaOx is still active), the presence of active enzyme in the soak buffer also suggests desorption from the surface over time and one of the factors to the likely loss of signal over time (Figs. 7 & 8). While the GaOx still adsorbed remains active toward galactose, there is an overall loss in the relative fluorescence over the course of 6 days (Supporting Information, Fig. SI-10). This enzyme loss is relatively unsurprising as enzyme leeching even from biosensing platforms that encapsulate enzymes (e.g., sol-gels, chitosan) is often observed and the use of semi-permeable membranes (e.g., polyurethane) to decrease this effect is also common [7, 22-24, 29].

Additional fluorescence assay for enzyme kinetics were performed on entire films of Au/CYST-SAM/COOH-SWCNT/GaOx systems as well as control films with denatured GaOx and with no GaOx adsorbed at the interface. Films were immersed in a six-well plate with Amplex Red and HRP before galactose substrate (10 mM) was added to initiate Reactions 2 and 3 above. The opaque 6-well plate containing whole films (see Supporting Information, Fig. SI-11A) was then monitored for fluorescence (i.e., peroxide production) in real-time after introduction of the substrate. This type of experiment was performed on films that were constructed on entire gold slides (film area  $\sim 1.74 \text{ cm}^2$ ; whole slide) as well as on films that were constructed within the electrochemical cells (film area  $\sim 0.32 \text{ cm}^2$ ; area defined by o-ring) and then transferred to the 6-well plate. Fluorescence production from the larger area films are shown in **Figure 9B** where the signal during exposure to 10 mM galactose rapidly increases over time toward saturation – a trend clearly distinguishable from both the denatured GaOx and no GaOx controls which, in relative comparison, yield nearly negligible signal. The first 180 seconds of data was modeled for determination of initial rate constants of  $22100_{(t=180)} \text{ s}^{-1}$  and  $3330_{(t=170)} \text{ s}^{-1}$  for the COOH-SWCNT platforms with native and denatured GaOx adsorbed, respectively. These same trends are mirrored in the results from the films removed from the electrochemical cells (Supporting Information, Fig. SI-11B). Again, essentially no activity recorded for both the film without GaOx and the film with previously denatured GaOx. Initial rate constants for these films were determined to be  $2770_{(t=420)} \text{ s}^{-1}$  and  $-400_{(t=290)} \text{ s}^{-1}$  for the COOH-SWCNT platforms with native and denatured GaOx adsorbed,

respectively. These assay results are in agreement with the fluorescent data collected from aliquot samples taken from the electrochemical cells (Fig. 9A) and suggest that the adsorbed GaOx remains active at the interface and is not denatured.

For an amperometric response to corroborate the results of the enzyme activity fluorescent assays, the same membranes used to decrease leeching from biosensing systems, can also be used to help capture of peroxide production in the presented platforms electrochemically, though it should be recognized that the assay is significantly more sensitive. Membranes at the solution interface of adsorption platforms serve to retain both the enzyme as well as hydrogen peroxide that is generated from the enzymatic reaction. Without a barrier of this nature, peroxide generated by the reaction is free to diffuse away into bulk and only a fraction of the peroxide will be oxidized at the electrode – a particular issue with platforms that have only thin layers of adsorbed enzyme. The Au/CYST-SAM/COOH-SWCNT/GaOx system held under an oxidizing potential and subjected to injections of galactose (1 mM) revealed no substantial current change during injections. When the same system is capped with a semi-permeable membrane of polyurethane, each injection resulted in a current change attributed to peroxide oxidation. The current observed at injection is small, as expected for a thin layer of enzyme capped with additional membrane suppression, but is also nonexistent in the absence of the GaOx – additional evidence of adsorbed enzyme activity (Supporting Information, Fig. SI-12 vs. SI-13). Thus, while these platforms are of interest fundamentally, for the purposes of using them in biosensors, the materials should be combined in a scaffold that allows for multi-layers of GaOx to enhance signal.

As in prior reports studying enzymes immobilized at electrode interfaces [4, 46], the presence of electrocatalytic reduction of oxygen was investigated for the composite films of this study. Au/CYST-SAM/COOH-SWCNT/GaOx films were constructed and the voltammetry observed under both aerobic and anaerobic conditions for systems with and without galactose substrate present. The results, shown in Supporting Information (Fig. SI-14), show the redox peaks attributed to the adsorbed GaOx, the copper-related redox reaction described in Rxn 1, are clearly observable in the presence and absence of oxygen. These results also show that the onset of oxygen reduction is observed at a more positive potential with the GaOx enzyme adsorbed to the composite film, i.e., versus the background. The shift in potential for oxygen reduction is similar in magnitude to what is reported in studies of GaOx at nanoparticle interfaces [4] as well as trends seen in studies

of films with immobilized glucose oxidase [46] and suggests that the immobilized GaOx in our system is capable of catalytic reduction of oxygen as well. Prior to obtaining this voltammetry all the solutions were scrubbed with catalase agarose beads to eliminate any residual peroxide from contributing to the electrochemistry.

The systems were also probed for bioelectrocatalysis capability where the GaOx directly oxidizes galactose substrate under anaerobic conditions [47]. First, cyclic voltammetry of the Au/CYST-SAM/COOH-SWCNT/GaOx system with/without oxygen and in the presence galactose. The results show that while the voltammetric peaks attributed to the copper core of GaOx are still observable once galactose is added to a system under anaerobic conditions, they have decreased in magnitude and exhibit a slight increase in peak splitting ( $\Delta E_p$ ) of ~16-20 mV (see Supporting Information, Fig. SI-15A). These same effects are observed when the systems are deoxygenated and experiments performed in the presence of catalase enzyme (1  $\mu$ M) to scavenge any hydrogen peroxide inadvertently produced via Rxn. 2 (Supporting Information, Fig. SI-15B). We note that similar results were achieved for the Au/CYST-SAM/COOH-SWCNT/GaOx system under both aerobic and anaerobic conditions in the presence of galactose, suggesting redox chemistry is occurring at the electrode stemming from GaOx reactions with galactose substrate (Supporting Information, Fig. SI-16). In a prior study [47], a similar experiment with the glucose oxidase showed identical voltammetry before and after the addition of glucose, a result investigators interpreted as negating the possibility of direct electron transfer involving glucose oxidase; the comparison is limited, however, since glucose oxidase requires an FAD cofactor that exhibits a voltammetric response while GaOx is a metalloenzyme that relies on copper.

In order to assess the bioelectrocatalysis potential of the Au/CYST-SAM/COOH-SWCNT/GaOx system, which is also known as a 3<sup>rd</sup> generation or direct biosensing mechanism, amperometric measurements under strict anaerobic conditions were conducted during systematic injections of galactose substrate. All the solutions were scrubbed for hydrogen peroxide with agarose catalase beads for 30 minutes prior to use. All of the solutions used were extensively degassed with nitrogen prior to these experiments. During injections of galactose at the electrodes featuring the Au/CYST-SAM/COOH-SWCNT/GaOx systems (and control film without enzyme), a continuous flow of nitrogen was bubbled into the solution to maintain a continuous O<sub>2</sub>-free environment. In the absence of oxygen, each injection of galactose substrate elicits an

amperometric response showing an oxidative current (Supporting Information, Fig. SI-17). This type of amperometric response is still observed upon the injection of galactose at the films in the presence of catalase in solution, suggesting that they are likely not due to peroxide generation. These results suggest that GaOx adsorbed to these platforms may also, have potential for utilization in 3<sup>rd</sup> generation or “direct” biosensing schemes though, when the overall study is considered, the use of the platforms in a 1<sup>st</sup> generation strategy or indirect biosensing scheme presents more advantages.

#### **4.0 Conclusions.**

PME continues to serve as a fundamental tool for studying the ET properties of metalloenzymes and metalloproteins. Increased understanding of the adsorbed electrochemistry of these enzymes and their activity at the adsorption platform can help inform the design and development of future biosensors. Indeed, the development of viable and clinically relevant 1<sup>st</sup> generation biosensors hinges on a fundamental understanding of the adsorption and function of biomolecules at synthetic interfaces. The adsorption of enzymes at SAM-modified electrodes, a platform that has found success for decades, exhibits inherent limitations for certain enzymes and proteins. In more recent years, studies have expanded to the use of nanomaterial-based adsorption platforms capable of promoting ET over greater distances [24, 25] and with more stability while maintaining enzymatic activity toward targeted substrate. In this study, we have explored the ET properties of copper core redox center in the GaOx enzyme at interfaces incorporating nanomaterials, most notably CNTs. Although the copper-based ET of GaOx has been notoriously difficult to observe at SAM-modified electrodes [34], the same interfaces amide-coupled to functionalized CNTs resulted in robust adsorption platforms for GaOx and allowed for readily observable cyclic voltammetry of the copper core. While a number of different CNTs were studied, the use of COOH-SWCNT was optimal, promoting ET over a greater distance without decay and producing stable voltammetry for over a week – a result attributed to greater electronic coupling between GaOx and the interface. Additionally, GaOx remains active at these platforms, exhibiting the electrocatalytic reduction oxygen and maintaining the ability to catalyze galactose to produce hydrogen peroxide – a phenomenon not achieved in prior studies with GaOx interfaces with gold NP platforms [4]. While peroxide production forms the fundamental basis of 1<sup>st</sup>

generation or “indirect” biosensors, the adsorption platform also responds to galactose under anaerobic conditions, suggesting that they could be employed in future studies focused on 3<sup>rd</sup> generation or “direct” biosensing designs. Understanding these materials and their properties represents a fundamental step of using CNT platforms as a functional component of biosensors, including those designed for galactose (detection of galactosemia) [48], sarcosine (prostate cancer) [29] and others [49].

### **Acknowledgements.**

The research was generously supported by the National Science Foundation (CHE-1401593), Virginia’s Commonwealth Health Research Board (MCL), the Beckman Foundation (MJP/MCL, NL/JAP), as well as the Camille & Henry Dreyfus Foundation (MCL) and the Floyd D. and Elisabeth S. Gottwald Endowed Chair of Chemistry (MCL). Funding from the National Institute of General Medical Sciences, National Institutes of Health (P20GM103499 - SC INBRE) is also recognized (WSC). We would like to thank Dr. Mariama Rebello de Sousa Dias (Department of Physics) and Ms. Christine Lacy (Director of Microscopy and Imaging) at the University of Richmond for ellipsometry and cross-sectional TEM measurements, respectively.

### **References**

- [1] A. El Kasmi, J.M. Wallace, E.F. Bowden, S.M. Binet, R.J. Linderman, Controlling Interfacial Electron-Transfer Kinetics of Cytochrome c with Mixed Self-Assembled Monolayers. *J. Amer. Chem. Soc.* 120 (1998) 225-6.
- [2] M. Collinson, E.F. Bowden, M.J. Tarlov, Voltammetry of covalently immobilized cytochrome c on self-assembled monolayer electrodes. *Langmuir* 8 (1992) 1247-50.
- [3] A.F. Loftus, K.P. Reighard, S.A. Kapourales, M.C. Leopold, Monolayer-Protected Nanoparticle Film Assemblies as Platforms for Controlling Interfacial and Adsorption Properties in Protein Monolayer Electrochemistry. *J. Amer. Chem. Soc.* 130 (2008) 1649-61.
- [4] J.M. Abad, M. Gass, A. Bleloch, D.J. Schiffrin, Direct Electron Transfer to a Metalloenzyme Redox Center Coordinated to a Monolayer-Protected Cluster. *J. Amer. Chem. Soc.* 131 (2009) 10229-36.
- [5] I.E. Sendroiu, D.J. Schiffrin, J.M. Abad, Nanoparticle Organization by a Co(II) Coordination Chemistry Directed Recognition Reaction. *J. Phys. Chem. C* 112 (2008) 10100-7.
- [6] S. Oscarsson, Factors affecting protein interaction at sorbent interfaces. *J. Chromatogr. B: Biomed Sci. Appl.* 699 (1997) 117-31.
- [7] M.H. Schoenfisch, K.A. Mowery, M.V. Rader, N. Baliga, J.A. Wahr, M.E. Meyerhoff, Improving the Thromboresistivity of Chemical Sensors via Nitric Oxide Release: Fabrication and in Vivo Evaluation of NO-Releasing Oxygen-Sensing Catheters. *Anal. Chem.* 72 (2000) 1119-26.
- [8] Q. Chi, J. Zhang, J.E.T. Andersen, J. Ulstrup, Ordered Assembly and Controlled Electron Transfer of the Blue Copper Protein Azurin at Gold (111) Single-Crystal Substrates. *J. Phys. Chem. B* 105 (2001) 4669-79.
- [9] D. Alvarez-Paggi, M.A. Castro, V. Tórtora, L. Castro, R. Radi, D.H. Murgida, Electrostatically Driven Second-Sphere Ligand Switch between High and Low

- Reorganization Energy Forms of Native Cytochrome c. *J. Amer. Chem. Soc.* 135 (2013) 4389-97.
- [10] J. Willit, E.F. Bowden, Adsorption and redox thermodynamics of strongly adsorbed cytochrome c on tin oxide electrodes. *J Phys. Chem.* 94 (1990) 8241-6.
- [11] Garber EAE, Margoliash E. Interaction of cytochrome c with cytochrome c oxidase: An understanding of the high- to low-affinity transition. *Biochim. Biophys Acta (BBA) - Bioenerg* 1015 (1990) 279-87.
- [12] R.K. Shervedani, M.S. Foroushani, Comparative electrochemical behavior of proteins; cytochrome c, agaricus bisporus laccase, and glucose oxidase, immobilized onto gold-thiol self-assembled monolayer via electrostatic, covalent, and covalent coordinate bond methods. *Electrochim. Acta* 187 (2016) 646-54.
- [13] V. Alizadeh, M.A. Mehrgardi, M. Fazlollah Mousavi, Electrochemical investigation of cytochrome c immobilized onto self-assembled monolayer of captopril. *Electroanalysis* 25 (2013) 1689-96.
- [14] R.V. Jagadeesh, V. Lakshminarayanan, Adsorption kinetics of phosphonic acids and proteins on functionalized Indium tin oxide surfaces using electrochemical impedance spectroscopy. *Electrochim Acta* 197 (2016) 1-9.
- [15] E. Lebègue, H. Smida, T. Flinois, V. Vié, C. Lagrost, F. Barrière, An optimal surface concentration of pure cardiolipin deposited onto glassy carbon electrode promoting the direct electron transfer of cytochrome-c. *J. Electroanal. Chem.* 808 (2018) 286-92.
- [16] I. Ashur, A.K. Jones, Immobilization of azurin with retention of its native electrochemical properties at alkylsilane self-assembled monolayer modified indium tin oxide. *Electrochim. Acta* 85 (2012) 169-74.
- [17] Hamzehloei A, Bathaie SZ, Mousavi MF. Probing redox reaction of azurin protein immobilized on hydroxyl-terminated self-assembled monolayers with different lengths. *J. Electroanal. Chem.* 755 (2015) 27-38.
- [18] M. Sezer, J-J. Feng, H.K. Ly, Y. Shen, T. Nakanishi, U. Kuhlmann, P. Hildebrandt, H. Möhwald, I.M. Weidinger, Multi-layer electron transfer across nanostructured Ag-SAM-Au-SAM junctions probed by surface enhanced Raman spectroscopy. *Phys. Chem. Chem. Phys.* 12 (2010) 9822-9.
- [19] J. Chovelon, M. Provence, N. Jaffrezic-Renault, S. Alexandre, J. Valleton, Transfer of mixed protein-fatty acid LB films onto Si/SiO<sub>2</sub> substrates. Influence of the surface free energy. *Mater. Sci. Eng. C* 22 (2002) 79-85.
- [20] CF. Blanford, RS. Heath, FA. Armstrong, A stable electrode for high-potential, electrocatalytic O<sub>2</sub> reduction based on rational attachment of a blue copper oxidase to a graphite surface. *Chem Comm* (2007) 1710-2.
- [21] TD. Rapson, U. Kappler, PV. Bernhardt, Direct catalytic electrochemistry of sulfite dehydrogenase: mechanistic insights and contrasts with related Mo enzymes. *Biochim Biophys Acta (BBA)-Bioenerg* 1777 (2008) 1319-25.
- [22] G.E. Conway, R.H. Lambertson, M.A. Schwarzmann, M.J. Pannell, H.W. Kerins, K.J. Rubenstein, J.D. Dattelbaum, M.C. Leopold, Layer-by-layer design and optimization of xerogel-based amperometric first generation biosensors for uric acid. *J. Electroanal. Chem.* 775 (2016) 135-45.
- [23] N.G. Poulos, J.R. Hall, M.C. Leopold, Functional Layer-By-Layer Design of Xerogel-Based First-Generation Amperometric Glucose Biosensors. *Langmuir* 31 (2015) 1547-55.

- [24] M.L. Vargo, C.P. Gulka, J.K. Gerig, C.M. Manieri, J.D. Dattelbaum, C.B. Marks, N.T. Lawrence, M.C. Leopold, Distance Dependence of Electron Transfer Kinetics for Azurin Protein Adsorbed to Monolayer Protected Nanoparticle Film Assemblies. *Langmuir* 26 (2010) 560-9.
- [25] M.H. Freeman, J.R. Hall, M.C. Leopold, Monolayer-Protected Nanoparticle Doped Xerogels as Functional Components of Amperometric Glucose Biosensors. *Anal. Chem.* 85 (2013) 4057-65.
- [26] C. González-Gaitán, R. Ruiz-Rosas, E. Morallon, D. Cazorla-Amorós, Effects of the surface chemistry and structure of carbon nanotubes on the coating of glucose oxidase and electrochemical biosensors performance. *RSC Adv.* 7 (2017) 26867-78.
- [27] M.B. Wayu, J.E. King, J.A. Johnson, C.C. Chusuei, A Zinc Oxide Carbon Nanotube Based Sensor for In Situ Monitoring of Hydrogen Peroxide in Swimming Pools. *Electroanalysis* 27 (2015) 2552-8.
- [28] M.B. Wayu, L.T. DiPasquale, M.A. Schwarzmann, S.D. Gillespie, M.C. Leopold, Electropolymerization of  $\beta$ -cyclodextrin onto multi-walled carbon nanotube composite films for enhanced selective detection of uric acid. *J. Electroanal. Chem.* 783 (2016) 192-200.
- [29] M.J. Pannell, E.E. Doll, N. Labban, M.B. Wayu, J.A. Pollock, M.C. Leopold, Versatile sarcosine and creatinine biosensing schemes utilizing layer-by-layer construction of carbon nanotube-chitosan composite films. *J. Electroanal. Chem.* 814 (2018) 20-30.
- [30] N. Hernández-Ibáñez, L. García-Cruz, V. Montiel, C.W. Foster, C. E. Banks, J. Iniesta, Electrochemical lactate biosensor based upon chitosan/carbon nanotubes modified screen-printed graphite electrodes for the determination of lactate in embryonic cell cultures. *Biosens Bioelectron* 77 (2016) 1168-74.
- [31] M. M. Barsan, M.E. Ghica, C.M. Brett, Electrochemical sensors and biosensors based on redox polymer/carbon nanotube modified electrodes: a review. *Anal. Chim. Acta* 881 (2015) 1-23.
- [32] M.T. Meredith, M. Minson, D. Hickey, K. Artyushkova, D.T. Glatzhofer, S.D. Minter, Anthracene-Modified Multi-Walled Carbon Nanotubes as Direct Electron Transfer Scaffolds for Enzymatic Oxygen Reduction. *ACS Catal* 1 (2011) 1683-90.
- [33] X. Luo, M. Brugna, P. Tron-Infossi, M.T. Giudici-Ortoni, É. Lojou. Immobilization of the hyperthermophilic hydrogenase from *Aquifex aeolicus* bacterium onto gold and carbon nanotube electrodes for efficient H<sub>2</sub> oxidation. *J Biol Inorg Chem* 14 (2009) 1275-88.
- [34] S. Shleev, J. Tkac, A. Christenson, T. Ruzgas, A.I. Yaropolov, J.W. Whittaker, L. Gorton, Direct electron transfer between copper-containing proteins and electrodes. *Biosens Bioelectron* 20 (2005) 2517-54.
- [35] J. Tkac, J.W. Whittaker, T. Ruzgas, The use of single walled carbon nanotubes dispersed in a chitosan matrix for preparation of a galactose biosensor. *Biosens. Bioelectron.* 22 (2007) 1820-4.
- [36] J. Haladjian, P. Bianco, F. Nunzi, M. Bruschi, A permselective-membrane electrode for the electrochemical study of redox proteins. Application to cytochrome c552 from *Thiobacillus ferrooxidans*. *Anal. Chim. Acta* 289 (1994) 15-20.
- [37] H.V. Hsieh, Z.A. Pfeiffer, T.J. Amiss, D.B. Sherman, J.B. Pitner, Direct detection of glucose by surface plasmon resonance with bacterial glucose/galactose-binding protein. *Biosens Bioelectron* 19 (2004) 653-60.

- [38] J-S. Jeong, H-J. Kwon, H-R. Yoon, Y-M. Lee, T-Y. Choi, S-P. Hong, A pulsed amperometric detection method of galactose 1-phosphate for galactosemia diagnosis. *Anal. Biochem.* 376 (2008) 200-5.
- [39] A.R. Schmidt, NDT. Nguyen, M.C. Leopold, Nanoparticle Film Assemblies as Platforms for Electrochemical Biosensing—Factors Affecting the Amperometric Signal Enhancement of Hydrogen Peroxide. *Langmuir* 29 (2013) 4574-83.
- [40] D. Bartczak, A.G. Kanaras, Preparation of Peptide-Functionalized Gold Nanoparticles Using One Pot EDC/Sulfo-NHS Coupling. *Langmuir* 27 (2011) 10119-23.
- [41] E. Laviron, General Expression of the Linear Potential Sweep Voltammogram in the Case of Diffusionless Electrochemical Systems. *J. Electroanal. Chem.* 101 (1979) 19-28.
- [42] J.M. Abad, SFL. Mertens, M. Pita, V.M. Fernández, D.J. Schiffrin, Functionalization of Thioctic Acid-Capped Gold Nanoparticles for Specific Immobilization of Histidine-Tagged Proteins. *J. Amer. Chem. Soc.* 127 (2005) 5689-94.
- [43] M.A. Hamon, J. Chen, H. Hu, Y. Chen, M.E. Itkis, A.M. Rao, P.C. Eklund, R.C. Haddon, Dissolution of Single-Walled Carbon Nanotubes. *Adv. Mater.* 11 (1999) 834-40.
- [44] A. Lakshmi, G. Gopu, S. Thanikaikarasan, T. Mahalingam, P. Alvarez, P.J. Sebastian, C. Vedhi, Electroanalysis of Diazepam on Nanosize Conducting Poly (3-Methylthiophene) Modified Glassy Carbon Electrode. *J. New Mater. Electrochem. Sys.* 17 (2014) 185-190.
- [45] RA. Clark, EF. Bowden, Voltammetric Peak Broadening for Cytochrome c/Alkanethiolate Monolayer Structures: Dispersion of Formal Potentials. *Langmuir* 13 (1997) 559-65.
- [46] X. Wu, F. Zhao, J.R. Varcoe, A.E. Thumser, C. Avignone-Rossa, R.C.T. Slade, Direct Electron Transfer of Glucose Oxidase Immobilized In An Ionic Liquid Reconstituted Cellulose-Carbon Nanotube Matrix. *Bioelectrochemistry* 77 (2009) 64-68.
- [47] M. Wooten, S. Karra, M. Zhang, W. Gorski, On the Direct Electron Transfer, Sensing, and Enzyme Activity in the Glucose Oxidase/Carbon Nanotubes System. *Anal. Chem.* 86 (2014) 752-757.
- [48] B. Dalkıran, P.E. Erden, E. Kılıç, Electrochemical biosensing of galactose based on carbon materials: graphene versus multi-walled carbon nanotubes. *Anal. Bioanal. Chem.* 408 (2016) 4329-39.
- [49] W. Putzbach, N. J. Ronkainen, Immobilization techniques in the fabrication of nanomaterial-based electrochemical biosensors: A review. *Sensors* 13 (2013) 4811-40.